www.gondwanags.org.in

Research Article

ISSN : 2455-1953

JGSR
Journal of Geosciences Research
Vol. 11, No.1, January, 2026, pp. 13-22

An Appraisal of Microstructures and Deformation Temperature in a Fold and Its Implications for the Structural Context of the Area Around Bagalkot, Karnataka, India

Chetan. P. Hanji [1,2*], A. Sreenivasa[2] and Anant. G. Pujar[2]

[1]*Department of Geology, Maharani's Science College for Women, Mysore 570005(KN), India*
[2]*Department of Studies in Geology, Karnatak University, Dharwad-580003 (KN), India*
*(*Corresponding Author, E-mail:chetanhpk@gmail.com)*

Abstract

The study investigates the tectonothermal history of a WNW-ESE trending fold system within the Proterozoic southern Kaladgi basin, India, an area where such analysis has been previously limited. Through detailed microstructural analysis of ten oriented quartzite samples using petrographic microscopy, we correlate observed deformation features with established experimental data to constrain the paleo-deformation conditions. The analysis identified a suite of recovery and recrystallization microstructures in quartz and feldspar grains, including bulging grain boundaries (BLG), sub-grain rotation (SGR), grain boundary migration (GBM), and chessboard extinction. These features constrain the average deformation temperature to a low-to-medium range of 300°C to 580°C, corresponding to lower-middle greenschist to lower amphibolite facies conditions. Higher temperatures are consistently localized in zones of increased strain, such as vicinity of faults, shears, and fold limbs. Fabric analysis and shear-sense indicators reveal a multi-stage deformation history driven by compressional forces, oriented NE-SW and N-S, which was overprinted by a significant NW-SE transpressional shear regime. By linking micro-scale evidence to the regional stress field, this research provides a comprehensive model for the basin's structural evolution, offering crucial insights for tectonic reconstructions and resource exploration.

Keywords: Microstructures; Deformation temperature; Quartz; Grain boundary migration; Sedimentary basin; Proterozoic

Introduction

Intracratonic basins are surrounded by cratons and are found to be broad, shallow and saucer shaped. Many basins of North Africa, between Atlantic ocean and red sea, Illinois basin of America covering Indiana and Kentucky has similar complex tectonic deformation history of evolution, Tagus basin within Iberian microplate is a result of differential tectonic strain during alpine orogeny and west Siberian basin is one of the largest intracratonic basins in the world, like others it has a complex multiphase tectonic history and is poorly understood having a basement of metamorphic, folded rocks and platformal blocks. Even in Indian context we have basins like, Cudduppah, Vindhyan, Chattisgarh, Pranhita-Godavari *etc.* These basins all around the world seems to be similar in structural evolution and deformational characters as our study area (Goswami *et al.*, 2023).

Deformation occurs in episodes and, there is a possibility of several episodes of deformation in an area. Deformation in solid Earth materials, particularly microscale and megascale structures, has recently been a topic of immense interest. Penetrative structures in rocks have created a wide riveting research scope. This proved indispensably important in deciphering the structural evolution of an area (Sigue *et al.*, 2023; Mamtani, 2025). Rock deformation varies with depth, being brittle and temperature-independent near the surface but ductile under higher temperatures and pressures at greater depths. With sufficient pressure, temperature, and time, rocks undergo internal adjustments such as microfractures, dislocation movements, and creep mechanisms to accommodate strain. These processes stabilize mineral grains and produce structures that record deformation history. Microstructure analysis of minerals like quartz and feldspars provides insights into past tectonic disturbances by examining their optical features, textures, and structures. Low-grade conditions typically form brittle structures, whereas high-grade conditions produce ductile ones.

Considering above background knowledge, the southern fringe of the Kaladgi basin is chosen for investigation as it is structurally disturbed and substantially retains the pages from the past. Several important aspects of the basin and its evolution have been documented, particularly the deformation phases in basement evolution and the kinematics of the south-central sector (Mukherjee *et al.*, 2016; Mukherjee and Modak, 2017; Pillai and Kale, 2019; Pujar *et al.*, 2021; Hanji *et al.,* 2025). Nevertheless, a

(Received : 20 Decmber 2024 ; Revised Form Accepted : 26 October 2025)
https://doi.org/10.56153/g19088-024-0238-87

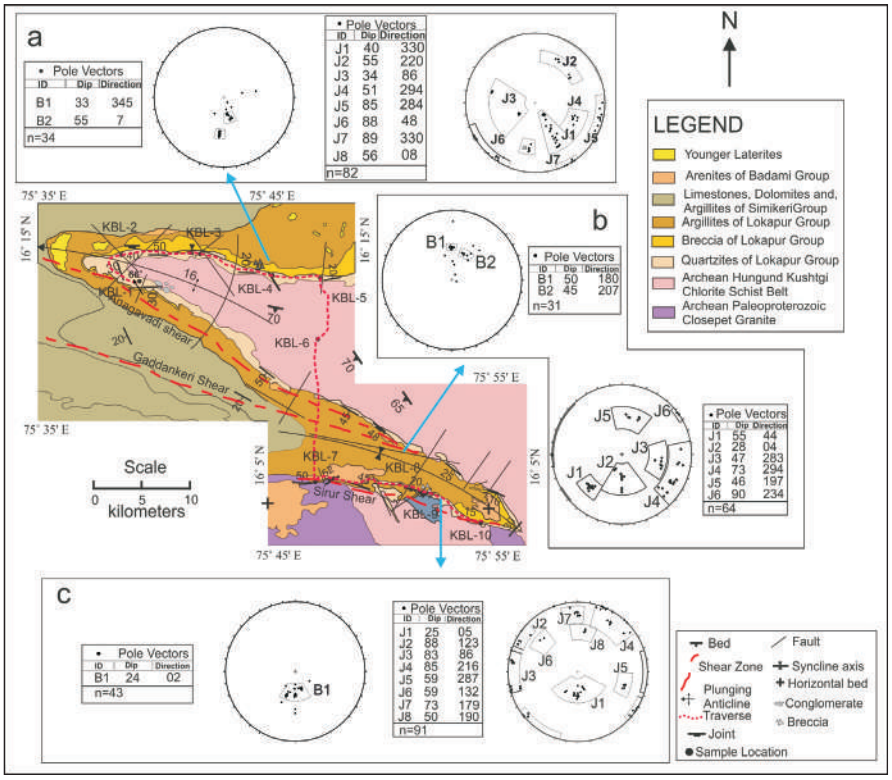

Fig.1. Synoptic map of the Study area showing the sampling sites along the traverse and other structural features and (a, b, c) shows the stereonet representation of structural data of the area divided into 3 domains (*after* Pillai and Kale, 2019, 2021)

comprehensive analysis of the microstructures in the southern part of the basin remains necessary to provide insights and to constrain deformation temperatures, a topic that has received limited attention in the literature. To the best of our knowledge, no dedicated study has yet been carried out on the microstructures and deformation temperatures of this area. This paper focuses on addressing the paucity of research in this domain of structural geology. The research primarily seeks to understand and establish, then analyse the structures by defining and studying distinct microstructures, linking the same with megascopic deformation trends and a possible derivation of an average temperature of the deformation from the literature and registered microstructures enabling the geological fraternity to have greater, deeper view and a new perspective towards the basin equipping in further research focusing on evolutionary studies along with mineral, hydrocarbon and hydrological exploration and geotechnical domains.

Geological Setting and Deformation Scenario

Archean rocks of peninsular India are overlain by Proterozoic basins such as Kaladgi and Bhima basins, separated by the remarkable Eparchean unconformity (Jayaprakash *et al.*, 1987). These intracratonic basins were possibly sinks for sediment deposition from surrounding terrain, resulting incyclic deposition of sediments and rock formations is evident throughout the basin (Pillai and Kale, 2019; Kale and Pillai, 2022). Kaladgi Supergroup is classified as lower Bagalkot group and upper Badami group. Badamis are less deformed compared to the lower Bagalkot formations (Jayaprakash, 2007).

According to (Mukherjee *et al*., 2016, 2019; Mukherjee and Modak, 2017) the basement forms the structural framework for Mesoproterozoic cover sediments. The basement rocks (Peninsular Gneissic Complex and Hungund Schist Belt) experienced three stages of deformation (D_1, D_2, and D_3). D1: Created tightly-folded, isoclinal F_1 folds. D_2: Refolded the F_1 folds, forming tight, non-cylindrical F_2 folds with steeply dipping axial surfaces and D_3: Caused broad, open, upright F_3 folds due to shortening along the NW–SE direction. The younger Closepet granite (*c.* 2.5 Ga) remained largely undeformed, while the Peninsular Gneissic Complex was deformed in phase with the Hungund Schist Belt. On other hand, the Mesoproterozoic cover sediments of the Kaladgi Basin underwent a single deformation event, likely caused by gravity gliding; might have triggered by a tectonic uplift of the basement during the Grenvillian Orogeny (*c.* 1000–800 Ma). According to the author this event decoupled the sedimentary cover from the basement, which remained unaffected by this younger deformation. The result was the development of WNW–ESE to E–W trending folds, strike-slip faults, and thrusts.

An alternative interpretation suggests the Kaladgi Basin's deformational history is marked by four distinct events: D_0, D_1, D_2, and D_3 (Pillai and Kale, 2019, 2021). D_0 and D_3 representing extensional tectonics, D_1, another Mesoproterozoic extensional phase, attributed to the reactivation of inherited basement shears, leading to basin reorganisation and D_2 signifying compressional deformation event that caused strong, tight folding and faulting of the Bagalkot Group and reactivation of basement shears. The authors, Patil Pillai and Kale, partially disagree with the gravity gliding model given by Mukherjee *et al*., (2016) for the folding in the Bagalkot Group. Instead, the authors propose that the folding and deformation are more plausibly explained by the reactivation of basement shears. They suggest that the large-amplitude,

WNW–ESE trending sinusoidal folds within the multilayered succession of the Bagalkot Group initially formed due to transpressional stresses oriented NE–SW and NW–SE during the D_2 deformational event. As the strain increased, this led to the development of sinistral and dextral verging cross-folds, associated with transverse fractures and followed by strike-slip faults. This model suggests that the inherited basement structures controlled the geometry and orientation of the deformation. Either way it is interpreted that the cover sediment deformation was a single-phase deformational event.

The present study area is one such significant fold system consisting of an anticline near Anagavadi and a syncline near Amingad of Bagalkot district, Karnataka, India, bordered by Archean gneiss and Hunagund-Kushtgi Schist Belt (HKSB) which are intruded by younger Closepet granite body.

The Northwest plunging anticline and southeast plunging syncline constitute this fold-system. We have picked the quartzites for this study to assess these structures as the quartz mineral grains are adept at accommodating and exhibiting microstructures. The anticline domain of the fold comprises the basal formation; Salagundi conglomerates overlain by Saundatti quartzites and breccia (Jayaprakash, 2007; Pillai and Kale, 2019). In contrast, the syncline domain has the same setup, except that the younger Badami Quartzarenites can be seen near the syncline closure bound by limbs, indicating deformation was before the deposition of the Badami Quartz arenite; the southern part (limb) of the syncline is in contact with Archean Banded Iron Formations (BIF) hosted by Hunagund-Kushtgi Schist Belt (HKSB), and Closepet Granite (Pillai and Kale, 2019; Fig. 1). The major minerals of the rocks are quartz, feldspar, and a small amount of mica. Several faults have formed orthogonal to the overall strike direction of the rocks (quartzite ridges), and the axial plane, because of differential basin uplift (Fig. 1) gravity sliding, and several subsequent deformation phases (Mukherjee *et al*., 2016; Pillai and Kale, 2021). Major displacements and disturbances have occurred in several areas such as the occurrence of boudinage at Herkal (Fig. 2e), slickensides at Yalligutti (Fig. 2b), quartz vein shear sense around Anagavadi (Fig. 2d), occurrence of a major shear zone near Kadlimatti (Fig. 2g), intense fracture development and shattering near Sirur (Fig. 2f), and Kamatgi (Fig. 2a, h). The area has undergone both brittle and ductile deformation and this must have certainly manifested penetrative microstructures, which are of immense interest.

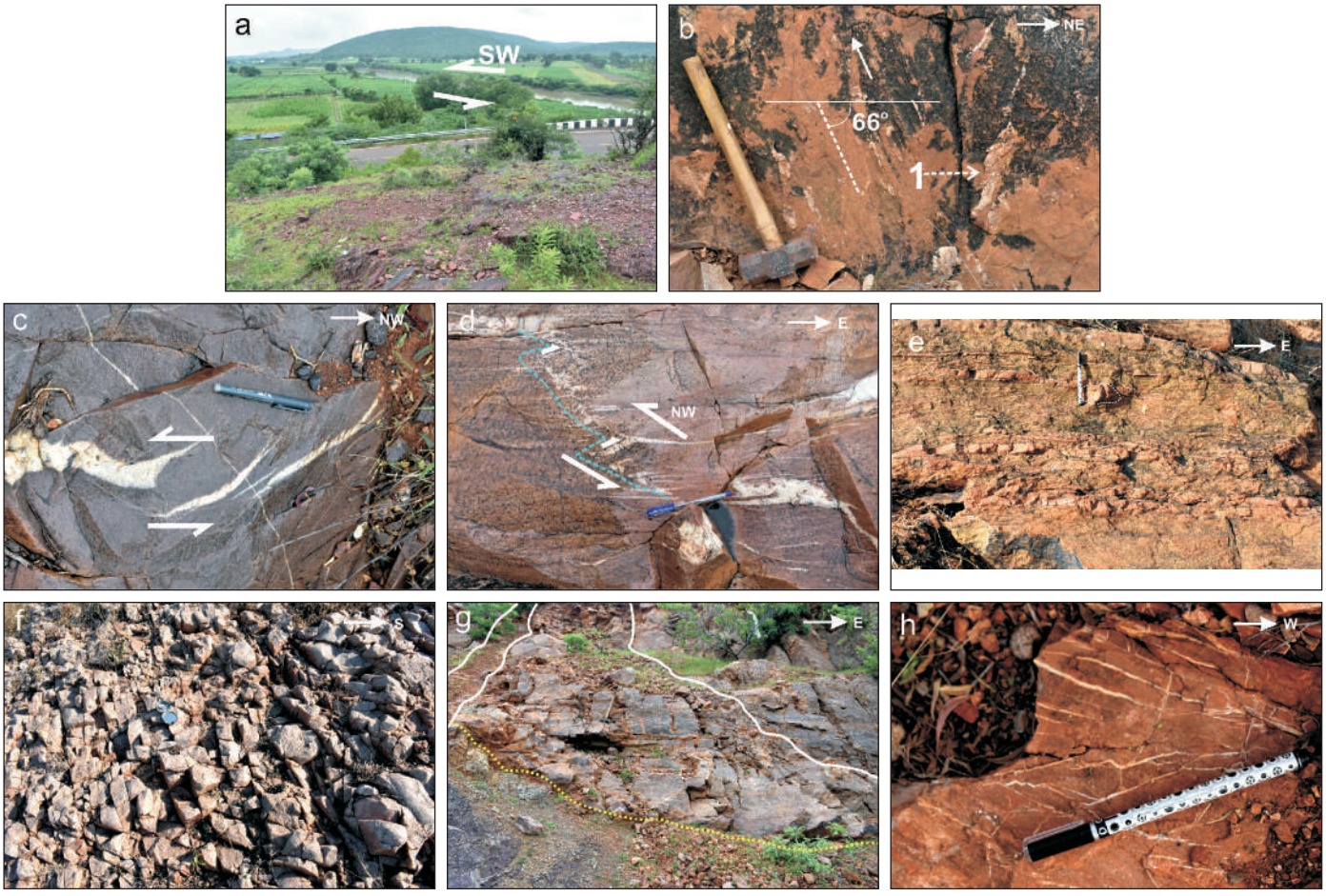

Fig.2. Field photographs showing structural features of the area(a) Major fault near Kamatgi village (KBL-9) with offset along SW direction; river flowing along the fault plane can be appreciated (b) Slickenside (trending NE) formed are appreciated well along the fault plane near Yelligutti village (KBL-1) with a sense of slip indicated by solid upward arrow. (c) Shearing induced tension gash structures formed in quartz vein trending NW-SE near Anagavadi village (KBL-2) (d) Shearing in quartz vein trending NW (e) Pinch and swell (necking) structures annotated indicates boudin formation in argillite interbedded quartzites near Herkal village (KBL-3) (f) Intense brittle fractures and shattering of quartzites formed near Sirur village (KBL-7) as an expression of a major shear zone running along the buttress of the basin (g) Shatter zone demarked horizontally by white continuous line and vertically by dotted yellow line in quartzites near Kadlimatti village, which may be a surficial expression of deep shear zone (KBL-5) (h) Recrystallised quartz in weak fractures due to intense shearing and cross-folding owing to the D2 deformation mentioned by Kale and Pillai, (2019). *(Pens measure 15cms, Hammer measures 46cms)*

Microstructures and Deformation Temperature

The study area is segmented into anticline and syncline sections for better comprehension. Ten oriented samples are acquired throughout the major fold, covering extensive part of it and designated as KBL-1 to KBL-10 along with field data and structures exposed (Fig. 2). Polished thin sections were prepared out of the samples at the Petrological Laboratory, Department of Studies in Geology, Karnatak University, Dharwad, India. High-resolution photomicrographs were obtained from the microscope and were analysed for deformational microstructures. The following paragraphs will elaborate on the technique and findings of the analysis. Detailed results are reported in Table 1. Among the ten samples (KBL-1 to KBL-10), six are classified under the anticline section; the remaining four are in the syncline part of the fold system.

Anticline portion of the fold system (from KBL-1 to KBL-5) have shown many microstructures registered in quartz and feldspar minerals (Fig. 3-4). Recovery microstructures like brittle fractures (microfractures), and undulose extinction (Fig. 3a-b) show very low-grade (<300°C) cataclastic deformation (Nishikawa and Takeshita, 1999) and, optically continuous syntaxial overgrowths support this interpretation (Fig. 3g). Deformation bands (indicating crystal plasticity) and undulose extinction show low-grade deformation conditions (300°C-400°C). A dynamic recrystallization structure, bulging grain boundary (BLG) (Fig. 3a; Stipp *et al.*, 2002) sometimes begin at a temperature below 300°C when quartz is much deformed (Wu and Groshong, 1991). Common microstructures across this regime are BLG, sub-grain boundary formation (Fig. 3b,d, and 4d), sub-grain rotation (SGR) (Lloyd and Freeman, 1994; Stipp *et al*., 2002) showing the moderate temperature of 400°C-500°C, and Grain boundary migration (Fig. 3e) (GBM, indicating complete sweeping of all dislocations and manifesting the grain to be strain-free by migrating boundaries and sub-grain boundaries) being typical of the high-temperature range of 500°C-700°C (Urai *et al*., 1986; Jessell, 1987; Stipp *et al*., 2002; Lychagin *et al.*, 2020). Additionally, KBL-1 shows peculiar chessboard extinction (Fig. 3b and 4c) forms at the same temperature (Blumenfeld *et al*., 1986; Mainprice *et al*., 1986; Stipp *et al*., 2002).

At low to medium temperature ranges of 400°C-500°C, deformation in feldspars is shown by bent twins, kink bands (Fig. 3f), grain scale dislocation glide-assisted micro-faults, undulose extinction and tapering deformation twins (Fig. 3e) being peculiar (Pryer, 1993; Ji, 1998a-b). At low metamorphic grade (<400°C), patchy extinctions occur due to smaller brittle fractures (Tullis and Yund, 1987). Sample KBL-6, collected from the strongly deformed and uplifted part of the HKSB within the study area, contains

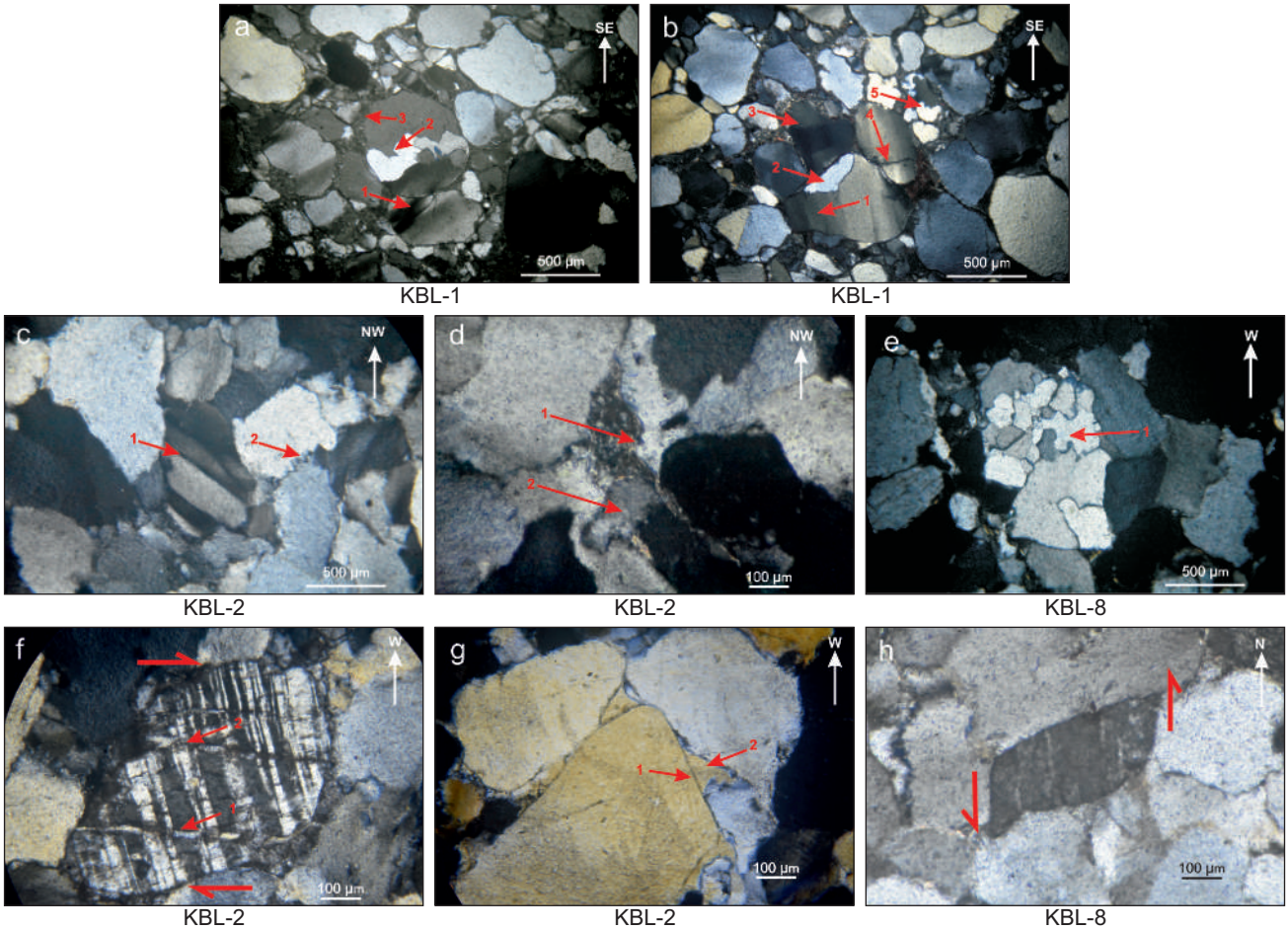

Fig.3. Photomicrographs (*under XPL unless mentioned specifically*) showing various microstructures (a) 1. Undulose extinction in quartz grain, 2. BLG, 3. Neocrystallisation around original quartz grain in the direction of minimal strain (b) 1. Undulose extinction in quartz grain, 2. Subgrain formed due to varied dislocation density, 3. Chessboard extinction in quartz, 4. Intragranular fractures to accommodate strain, 5. GBM (c) 1. Kink bands in quartz, 2. GBM (d) 1. Intergranular secondary mica filling, 2. Subgrain formation (e) 1. GBM and lobate boundaries in quartz (f) 1 and 2. Kink bands in feldspar grain due to shearing strain, intragrain fracture is also observed (g) 1. Original grain boundary in quartz, 2. Overgrowth of quartz grain across the original boundary (h) Shear in feldspar trending top-to-north

rhyolitic intrusives with subhedral quartz porphyroclasts (Fig. 4a) in fine-grained quartz matrix. The development of extensional crenulation cleavages (C′ planes) is also evident (Fig. 3i; Williams and Burr, 1994)). Feldspar and mica assemblages indicate a low- to medium-grade temperature regime (300–500 °C), and several microstructures display shear-sense indicators (Figs. 3f, h; 4b, f, h).

Conversely, Syncline possesses samples ranging from KBL-7 to KBL-10. Quartz exhibits inequigranular inter-lobate to polygonal grains, with strong SGR (Lloyd and Freeman, 1994; Stipp *et al.*, 2002), GBM (Jessell, 1987; Stipp *et al.*, 2002), and Chessboard extinction (Fig. 4c; Blumenfeld *et al.*, 1986; Mainprice *et al.*, 1986; Stipp *et al.*, 2002) observed along the Sirur shear zone and the Malaprabha River at Kamatagi, indicating elevated temperatures of 500°C-700°C. The brecciated sample KBL-9 has subangular smaller quartz grains, with quartz clasts displaying patchy undulose extinction indicative of a lower temperature regime (~300°C). Feldspars regularly exhibit bent twins, tapering twins (Fig. 4e), undulose extinction, and core-mantle structures (Fig. 4d) with minimal change in the upper medium temperature range of 450°C-600°C (Passchier and Trouw, 2005; Hentschel *et al.*, 2019). Additionally, according to the experimental data and classification provided by Hirth and Tullis, (1992), BLG is the main mechanism by which the quartzite sample deforms under Regime 1, SGR under Regime 2 and, GBM under Regime 3, and hence we can also be able to have a regime wise perspective for the deformation in the area. The temperature regime of the deformed area is characterised as medium to high for the anticline and low for the syncline segment, not forgetting that the samples falling on shears show high temperature features which might be due to the strain localization in the area as Shear zones are well known for localizing strain. The temperature profile over the area is well explained by multiple phases of deformation.

Results

Microstructural analysis was conducted to determine deformation mechanisms and corresponding temperatures. The comprehensive findings are summarized in Table 1 and detailed below.

Deformation Temperatures

The estimated deformation temperatures range from low to medium metamorphic conditions, with an average between 300°C and 580°C. Most samples fall within this range, though a few

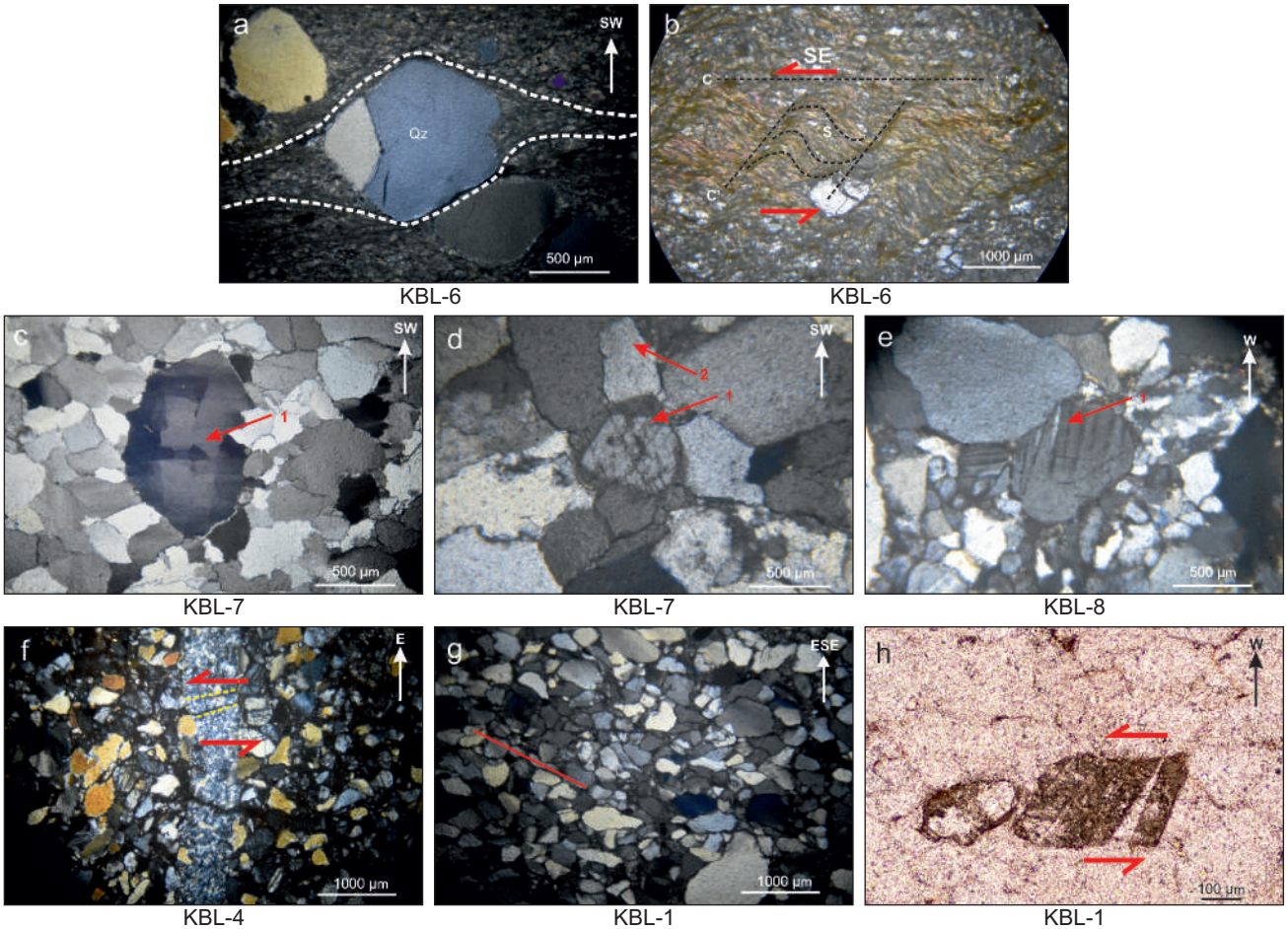

Fig.4. Photomicrographs (*under XPL unless mentioned specifically*) showing various microstructures (a) Quartz porphyroclast with strained beard structures around it (b) Extensional Crenulation Cleavage (ECC) defining C'-planes in meta rhyolite showing curved S planes and C planes trending SE (c) 1. Chessboard extinction in quartz (d) 1. Core and mantle structure in feldspar, 2. Subgrain formation in quartz (e) 1. Tapering deformation twins in feldspar grain (f) 1. Shear in quartz vein and subsequent micro-fault trending top-to-north (g) Strong shape preferred orientation marked by a line in quartz grains (h) V-parting in feldspar grain showing shear sense trending top-to-north (PPL)

Table 1: Detailed Microstructural Analysis, Optical properties of individual samples and interpretation of deformation temperature

SI. No	Sample ID	Location	Rock Type	Optical Properties	Deformation Temperature
1	KBL-1	16.231338 75.673461	Quartzite	Some quartz grains exhibit sweeping undulatory extinction. These grains are inequant with smooth boundaries, exhibiting subangular to subrounded and intergranular spaces filled with siliceous and ferruginous material. Intergranular mica deposits are present. Grains are dynamically recrystallized, a few of them have mica inclusions and substantial bulging grain boundary, sub grain rotation, chess board extinction and, core mantle structures are seen in few quartz grains.	At medium temperatures between 400°C and 500°C, dominant recrystallisation mechanism here is SGR recrystallisation (Lloyd and Freeman, 1994; Stipp *et al.*, 2002). At high grade conditions 500°C-700°C, recrystallisation is largely by GBM recrystallisation, grain boundaries are lobate, and pinning or migration microstructures (Jessell, 1987; Stipp *et al.*, 2002) are typical at lower temperature ranges. A unique sort of approximately square sub grain structure arises at these high-grade conditions, known as checkerboard extinction or chessboard sub grains which may be related to combined basal <a> and prism <c> slip (Blumenfeld *et al.*, 1986; Mainprice *et al.*, 1986; Stipp *et al.*, 2002) or the α-β transition in quartz (Kruhl, 1996).
2	KBL-2	16.252692 75.658385	Quartzite	Quartz grains exhibit sub-angular, inequant, crystalline nature. They also have kinks, bulging grain borders, sub grain development, rotation and, a few scattered deformation lamellae and intergranular mica. Dynamic recrystallization is pronounced by grain boundary migration in quartz grains. Laths of subhedral feldspar have secondary mica deposited in between grains and sealed fractures within.	A dominant dynamic recrystallisation mechanism under 400°C condition is BLG recrystallisation (Stipp *et al.*, 2002). At medium temperatures between 400°C and 500°C, dominant recrystallisation mechanism here is SGR recrystallisation (Lloyd and Freeman, 1994; Stipp *et al.*, 2002). Old grains may be wholly replaced by recrystallised material (Hirth and Tullis, 1992; Stipp *et al.*, 2002). At 500°C-700°C, recrystallisation is largely by GBM recrystallisation, grain boundaries are lobate, and pinning or migration microstructures (Jessell, 1987; Stipp *et al.*, 2002) are typical at lower temperature ranges. Grain boundaries are lobate or amoeboid in shape.
3	KBL-3	16.25450 75.713617	Quartzite	Under plane polarized light, quartz grains appear indistinguishable from their neighbours due to boundaries with low relief. They are big and almost equigranular subhedral (polygonal) with no intergranular voids between them, implying grain boundary area reduction. However, some quartz grains have bulging grain boundaries. A few of other quartz grains show Sub-grain formation. Grain boundary migration seems to be evident in few as well. Chess board pattern of extinction is also seen in few quartz grains. Less of subhedral feldspar laths are seen which arebent and have overgrowths. Feldspar grains encircled by quartz show undulose extinction.	At 500°C-700°C, recrystallisation is largely by GBM recrystallisation, grain boundaries are lobate, and pinning or migration microstructures (Jessell, 1987; Stipp *et al.*, 2002) are typical at lower temperature ranges. Grain boundaries are lobate or amoeboid in shape. A unique sort of approximately square sub grain structure arises at these high-grade conditions, known as checkerboard extinction or chessboard sub grains which may be related to combined basal <a> and prism <c> slip (Blumenfeld *et al.*, 1986; Mainprice *et al.*, 1986; Stipp *et al.*, 2002). 2. At low-medium grade circumstances (400°C-500°C) feldspar still deforms mainly via internal micro fracturing but is assisted by modest dislocation glide. Tapering deformation twins, bent twins, undulose extinction, deformation bands and kink bands with abrupt borders may be present (Ji, 1998a-b; Pryer, 1993)
4	KBL-4	16.238973 75.768345	Quartzite	Sample exhibits cataclastic and inequant quartz grains. Quartz vein intrusion with recrystallised micro-quartz is seen. Common in cataclastic quartz are intracrystalline impingement micro-fractures, they additionally display bulging grain boundaries, sub-grain formation and, undulatory extinction. In comparison to quartz, feldspar is more prone to fractures. Multiple quartz veins with ferruginous opaque matrix are observed and, deformation bands are frequently seen. Feldspars display displaced bent deformation Twin bands, cleavage planes. grain scale micro-faults are scattered over the thin section.	At temperatures below 300°C, the primary mechanisms of deformation are brittle fracturing, pressure solution, and solution transfer of material (Dunlap *et al.*, 1997; Stipp *et al.*, 2002; Van Daalen *et al.*, 1999). Characteristic structures include intragranular fractures, undulose extinction, kink bands (Nishikawa and Takeshita, 1999) and indications of pressure solution and redeposition of material, occasionally found in veins. Dislocation glide and creep become significant at low temperatures (300°C-400°C). A dominant dynamic recrystallisation mechanism under these conditions is BLG recrystallisation (Stipp *et al.*, 2002). At low metamorphic grade (below 400°C) feldspar deforms largely by brittle fracturing and cataclastic flow. The grain fragments reveal substantial intracrystalline deformation including grain scale faults and bent cleavage planes and twins.
5	KBL-5	16.238304 75.806514	Quartzite	There are no intergranular spaces between the quartz grains; there is closed contact with high angle borders (almost polygonal) in most of the grains, other quartz grains exhibit sweeping extinction, bulging grain boundaries. Overgrowths at boundaries filling intergranular voids and a few lobate boundaries, suggesting recrystallization by bulging grain boundary and grain boundary migration in quartz grains. Additionally, it shows kinks. Micro-quartz makes up the component of quartz vein intrusions, and deformation bands extend outward from impinging sites. There are pronounced elongated Quartz sub grain formation and rotation in quartz. Whereas feldspar grains exhibit bent cleavages, displacement in twin bands (grain scale micro-faults), core mantle structure in other grains.	At medium temperatures (400°C-500°C), Pressure solution may still play a role under these conditions (Brok, 1992). The dominant recrystallisation mechanism here is SGR recrystallisation (Lloyd and Freeman, 1994; Stipp *et al.*, 2002). At 500?-700°C, recrystallisation is mostly by GBM recrystallisation, grain boundaries are lobate, and pinning or migration microstructures are common (Jessell, 1987; Stipp *et al.*, 2002) at lower temperature ranges. Grain boundaries are lobate or amoeboid in shape. At low-medium grade conditions (400°C-500°C) feldspar still deforms mainly by internal micro fracturing but is assisted by minor dislocation glide. Tapering deformation twins, bent twins, undulose extinction, deformation bands and kink bands with sharp boundaries may be present (Ji, 1998a-b; Pryer, 1993).

Continued.....

..... Continued

SI. No	Sample ID	Location	Rock Type	Optical Properties	Deformation Temperature
6	KBL-6	16.192465 75.802551	Meta-Rhyolite	Quartz porphyroclasts are clearly visible throughout the rock and are encircled by a matrix of mica, feldspar, and micro-quartz. Quartz phenocrysts are entirely subhedral (hexagonal) lacking wavy extinction (strain free); few quartz grains exhibit strain shadows and beard structures, which clearly indicate shear sense. A small number of quartz phenocrysts exhibit a core mantle structure surrounded by recrystallized quartz. Peculiar S-C' fabrics can be seen along with ECC evident. There are also sporadic feldspar euhedral laths that clearly show their cleavages.	Deformed rhyolites are quartz-feldspar aggregates deformed at low to medium grade condition(300°C-500°C) rocks, at these conditions, quartz is weaker than feldspar mineral and phenocrysts are preserved as porphyroclasts (Fig. 3i; Williams and Burr, 1994). Grain boundary sliding or pressure solution favours deformation of fine-grained polymineralic matrix in rhyolites (Passchier and Trouw, 2005) Deformed rhyolites can be recognised by the presence of euhedral to subhedral quartz phenocrysts with typical wriggly embayment (Fig. 3i; Williams and Burr, 1994).
7	KBL-7	16.09372 75.802796	Quar-tzite	Quartz grains are in contact with each other, devoid of intergranular spaces. Grain boundary migration is seen in quartz grains, with almost ununiform grain boundaries; recrystallized grains are common. Quartz frequently exhibits sub grain rotation and significantly Grain boundary migration. A profound number of quartz grains have extinction pattern resembling chess board. Feldspar show twin deformation lamellae and distinct core mantle structures are seen along with sparse micas and pyroxene grains.	At 500°C-700°C, recrystallisation is mostly by GBM recrystallisation, grain boundaries are lobate (Jessell, 1987; Stipp *et al.*, 2002) at lower temperature ranges. Above 700°C, prism-slip {m} <c> becomes important (Blumenfeld *et al.*, 1986; Mainprice *et al.*, 1986) and rapid recrystallisation and recovery cause most grains to have a strain free appearance. Grain boundaries are lobate or amoeboid in shape. A special type of approximately square sub grain structure occurs at these high-grade conditions, known as chessboard extinction or chessboard sub grains (Fig. 3) which may be due to combined basal <a> and prism <c> slip (Blumenfeld *et al.*, 1986; Mainprice et al., 1986; Stipp *et al.*, 2002) or the α-β transition in quartz (Kruhl, 1996). At medium-grade conditions (450-600°C). (Borges and White, 1980; Gapais, 1989; Gates and Glover, 1989; Tullis and Yund, 1991) dislocation climb becomes possible in feldspars and recrystallisation starts to be important, especially along the edge of feldspar grains. Recrystallisation is mainly BLG by nucleation and growth of new grains This is visible in thin section by the development of mantles of fine-grained feldspar with a sharp boundary around cores of old grains, without transitional zones with sub grain structures; typical core-and-mantle structures develop (Passchier, 1982).
8	KBL-8	16.090268 75.865617	Quar-tzite	Quartz exhibits anhedral character. The intergranular infill is composed of ferruginous opaque material and preferentially mica. A few quartz grains exhibit intracrystalline fractures, bulging grain boundaries; grain boundary migration, lobate boundaries and sub-grain rotation are highly expressed. Tapering deformation twin lamellae are seen in feldspar grains, much of microcline with Tartan twinning has developed because of deformation. sweeping extinction. Bent feldspar and mica are also observed showing shear sense.	At medium temperatures between 400°C and 500°C, prism {m} slip becomes significant and dislocation creep predominates. Characteristic are generally highly flattened old crystals and numerous recoveries and, recrystallisation structures. The dominant recrystallisation mechanism here is SGR recrystallisation (Lloyd and Freeman, 1994; Stipp *et al.*, 2002) At 500°C-700°C, recrystallisation is largely by GBM recrystallisation, grain boundaries are lobate, Prism {m} <c> slip becomes significant beyond 700°C (Blumenfeld *et al.*, 1986; Mainprice *et al.*, 1986) and most grains seem strain-free because of quick recrystallization and recovery. At low-medium grade conditions (400°C-500°C) feldspar still deforms mainly by internal micro fracturing but is assisted by minor dislocation glide. Tapering deformation twins, bent twins, undulose extinction, deformation bands and kink bands with sharp boundaries may be present (Ji, 1998a-b; Pryer, 1993)
9	KBL-9	16.08697 75.875204	Quar-tzite	The quartz grains in the thin section are subangular to sub rounded and unsorted, quartz grains seem to be micro fractured and with very little undulose extinction. An opaque intragranular matrix fills in the voids which may be ferruginous. Micro-quartz is found to be present.	At temperatures below 300°C, the primary mechanisms of deformation are brittle fracturing, pressure solution, and solution transfer of material (Dunlap *et al.*, 1997; Stipp *et al*., 2002; Van Daalen *et al.*, 1999). Characteristic structures include intragranular fractures, undulose extinction, kink bands (Nishikawa and Takeshita, 1999) and indications of pressure solution and redeposition of material, occasionally found in veins.
10	KBL-10	16.064432 75.924151	Quar-tzite	Micro-quartz is recognizable; however, most quartz grains are smaller in size. There are relatively few big, anhedral quartz grains with kinks, bulging grain boundaries and sub grain rotation occurring as alternative narrow band. It is discovered that the matrix is made up of opaque ferruginous substance indicating solution activity. Few grains of feldspar with tapering twin lamellae and sweeping extinction are found along with sparse microcline.	At medium temperatures between 400°C and 500°C, prism {m} slip becomes significant and dislocation creep predominates. The dominant recrystallisation mechanism here is SGR recrystallisation (Lloyd and Freeman, 1994; Stipp *et al.*, 2002). At around 400°C, bulging grain boundaries are also common (Stipp *et al.*, 2002). At low-medium grade circumstances (400°C-500°C) feldspar still deforms mainly via internal micro fracturing but is assisted by modest dislocation glide. Tapering deformation twins, bent twins, undulose extinction, deformation bands and kink bands with abrupt borders may be present (Ji, 1998-b; Pryer, 1993).

isolated clasts exhibited microstructures indicative of very high temperatures, which are interpreted as transported material from provenance rocks. Samples KBL-4 and KBL-9 represent the lower end of the thermal spectrum, with temperatures estimated between 300°C and 400°C. Spatially, higher deformation temperatures correlate with zones of high strain, such as fault zones and the limbs of the fold system (Fig. 5).

Fabric and Grain Orientation

A strong Shape Preferred Orientation (SPO) of grains is evident across the samples. This alignment is generally parallel to the regional bedding strike (NW-SE), with some local deviations at an acute angle. The predominant grain elongation and orientation direction around faults is NE-SW. In contrast, sample KBL-8 exhibits concavo-convex quartz grain contacts with an E-W elongation. Secondary mineral growth (mica) and evidence of solution activity are primarily oriented parallel to NW-SE and E-W trends.

Microstructural Observations by Sample

Specific microstructures provide evidence for distinct deformation processes:

High-Temperature Deformation

Chessboard extinction patterns were observed in quartz grains from samples KBL-1 and KBL-7. KBL-1 also shows neocrystallisation of smaller quartz grains along a strong NW-SE SPO (Fig. 3a-b).

Dynamic Recrystallization

Grain boundary migration (GBM) is present in sample KBL-2, located near the fold hinge.

Shear Sense Indicators

Sinistral shear is indicated by feldspar fish in KBL-2 (Fig. 3h) and by offset veins and feldspar grains in KBL-4 (Fig. 4f). Kinks in feldspar grains within sample KBL-5 suggest shearing along a N-S trending fault plane (Fig. 3f). Extensional Crenulation Cleavage (ECC or S-C' fabric), overprinting a pre-existing NW-trending foliation, was identified in KBL-6 (Fig. 4b).

Brittle and Ductile Deformation

Sample KBL-3, from a boudinage structure, contains pinch-and-swell features and fractures orthogonal to layer-parallel extension (Fig. 2e). Sample KBL-5 is located in a zone of shattered quartzite with fractures filled by quartz, aligned with a NNE-SSW to N-S shear plane (Fig. 2g). Associated macrostructures for KBL-1 include tension gashes showing a sinistral sense of shear (Fig. 2c).

Porosity and Grain Contacts

Samples KBL-3, KBL-5, and KBL-7 exhibit near-zero porosity with tightly interlocking grain boundaries. Other samples show varying degrees of solution and precipitation features.

Discussion

Metamorphic Conditions and Crustal Depth

The observed microstructures and the average deformation temperature range of 300°C-580°C suggest deformation under lower–middle greenschist to lower amphibolite facies conditions (Faleiros *et al.*, 2010; Grujic *et al.*, 2011). Such temperatures are characteristic of mid-crustal deformation zones (Faleiros *et al.*, 2010; Simonetti *et al.*, 2021). The dominance of ductile features including grain boundary migration recrystallization, S-C′ fabrics, and folding over brittle faulting further supports deformation at depth (Grujic *et al.*, 2011; Papeschi and Musumeci, 2019). Finally, the occurrence of a peripheral brittle zone (*e.g.,* shattered quartzite in KBL-5) overlying ductile shear reflects the brittle–ductile interplay commonly reported in orogenic shear zones (Papeschi and Musumeci, 2019; Petroccia *et al.*, 2025).

Stress Fields and Tectonic Evolution

The microstructural data allows for the reconstruction of the paleo-stress field. The predominant NE–SW grain alignment is consistent with the initial N–S to NE–SW compressional stress that led to the transpressional buckling of cover sediments and the

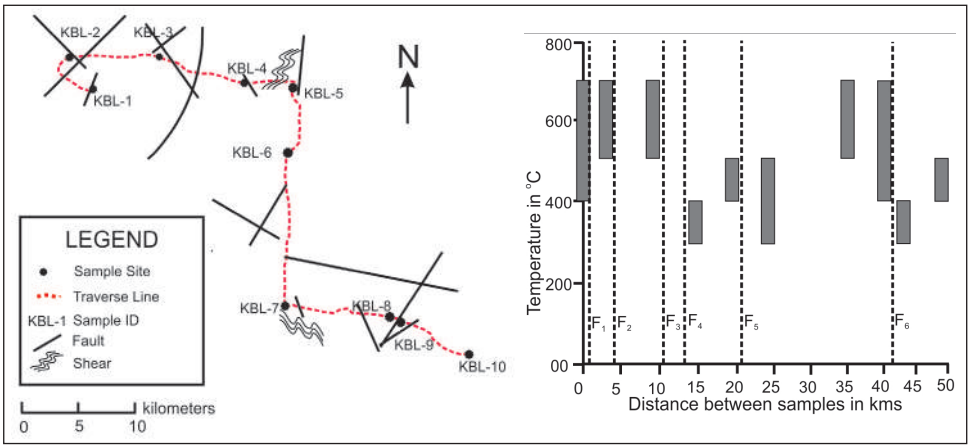

Fig.5. Map showing Traverse and Sampling sites, inset is the graph showing the variation of deformation temperature against the distance between the samples (Thin sections were analysed using EllipseFit Software V 3.11.0; Hanji *et al*., 2025)

primary fold generation, as proposed by Kale *et al.* (1998) and further elaborated by (Mukherjee *et al.*, 2016; Mukherjee and Modak, 2017; Pillai and Kale, 2019, 2021; Kale and Pillai, 2022). The coexistence of different fabric orientations points to a multi-stage or complex deformation history (Passchier and Trouw, 2005).

N–S Compression

The E–W elongation of grains in KBL-8, located near a southern Archean gneiss buttress, indicates a principal stress direction-oriented N–S, which is consistent with paleo stress analyses reported in similar tectonic settings (Saintot *et al.*, 2003).

NW-SE Transpression/Shear

The strong NW–SE SPO in KBL-1, along with sinistral shear indicators (KBL-2, KBL-4), points to a significant NW–SE oriented shearing component active during deformation, a feature comparable to other transpressional shear zones worldwide (Ezati *et al.*, 2022; Klepeis *et al*., 2022).

Extensional Regimes

The orientation of secondary minerals and solution activity parallel to the NW–SE to E–W direction marks these as axes of minimum strain (extension). Boudinage structures in KBL-3 provide clear evidence for localized extension, likely occurring at the intersection of fault systems within the overall transpressional setting (Armitage *et al.*, 2021).

Broader Implications

This study bridges the gap between micro-scale analysis and the macro-scale tectonic evolution of the fold system. By linking specific microstructures to deformation temperatures and stress orientations, we provide a detailed model of the strain distribution within the fold. These findings are crucial for tectonic reconstruction, correlating local deformation events with large-scale regional processes like plate convergence and transpressional movements (Kale *et al.,* 1998; Pillai and Kale, 2019, 2021; Kale and Pillai, 2022), and for resource exploration and geotechnical studies, where understanding the orientation of stress fields, fracture networks (*e.g.,* KBL-5 damage zone), and porosity distribution is essential for resource extraction and assessing rock mass stability (Passchier and Trouw, 2005)

Conclusions

This microstructural investigation successfully deciphered the complex tectonothermal history of the fold system. The analysis reveals that deformation occurred under mid-crustal conditions, with temperatures of 300°C−580°C corresponding to lower greenschist to lower amphibolite facies, promoting predominantly ductile deformation mechanisms. The results delineate a multi-stage stress regime, initiated by N-S to NE-SW compression responsible for the primary folding, which was subsequently overprinted and modified by a significant NW-SE transpressional shear component and localized extension. By integrating micro-scale evidence with macro-scale structures, this study provides a robust model of the region's tectonic evolution, offering critical insights that are valuable for both fundamental geological understanding and practical applications in resource exploration and geotechnical engineering.

Authors' Contributions

CPH: Investigation, Conceptualization, Methodology, Writing original draft. **AS:** Visualization, Supervision, Editing. **AGP:** Investigation, Conceptualization, Methodology, Supervision.

Conflict of Interests

The authors have no competing interests to declare regarding this article.

Acknowledgements

I would like to express my gratitude to the following individuals for their expertise, assistance, and motivation throughout all aspects of our study and for their help in writing the manuscript; Mr. Alok Hegde, Miss. Aishwarya Yadawad, Dr. Avinash Ammanagi, Mr. Ajit Hunashyal. We also express our sincere thanks to the reviewers and the Editor of the JGSR.

Funding

This work has received partial support in form of University Research Scholarship (PhD) offered by the Karnatak University, Dharwad. (Notification No: KVV/Scholarship/URS/2022/359 ,18/09/2022)

References

Armitage, T.B., Watts, L.M., Holdsworth, R.E. and Strachan, R.A. (2021). Late Carboniferous dextral transpressional reactivation of the crustal-scale Walls Boundary Fault, Shetland: the role of pre-existing structures and lithological heterogeneities. Jour. Geol. Soc. London, v. 178(1).

Blumenfeld, P., Mainprice, D., Tectonophysics and Bouchez, J.L. (1986). C-slip in quartz from sub-solidus deformed granite. Tectonophysics, v. 127(1–2), pp. 97–115.DOI:10.1016/0040-1951(86)90081-8

Borges, F.S. and White, S.H. (1980). Microstructural and chemical studies of sheared anorthosites, Roneval, South Harris. Jour. Struct. Geol., v. 2(1-2), pp. 273–280.

Brok, den B. (1992). An experimental investigation into the effect of water on the flow of quartzite. Utrecht.

Dunlap, W.J., Hirth, G. and Teyssier, C. (1997). Thermomechanical evolution of a ductile duplex. Tectonics, v. 16(6), pp. 983-1000.

Ezati, M., Rashidi, A., Gholami, E., Mousavi, S.M., Nemati, M., Shafieibafti, S. and Derakhshani, R. (2022). Paleostress Analysis in the Northern Birjand, East of Iran: Insights from Inversion of Fault-Slip Data. Minerals, v. 12(12), pp. 1606.

Faleiros, F.M., Campanha, G.A. da C., Bello, R.M. da S. and Fuzikawa, K. (2010). Quartz recrystallization regimes, c-axis texture transitions and fluid inclusion reequilibration in a prograde greenschist to amphibolite facies mylonite zone (Ribeira Shear Zone, SE Brazil). Tectonophysics, v. 485(1-4), pp. 193–214.

Gapais, D. (1989). Shear structures within deformed granites: mechanical and thermal indications. Geology, v. 17, pp. 1144–1147.

Gates, A.E. and Glover, L. (1989). Alleghanian tectono-thermal evolution of the dextral transcurrent hylas zone, Virginia Piedmont, USA. Jour. Struct. Geol., v. 11(4), pp. 407–419.

Goswami, S., Das, S., Samant, P.S., Kumar, T.V., Chakrabarti, K. and Prakash, B.G. (2023). Tectonic setting of Kaladgi-Badami basin and its possible connection with adjacent Proterozoic basins, Karnataka, India. Jour. Ind. Assoc. Sedimentolog., v. 40(I), pp. 55–72.

Grujic, D., Stipp, M. and Wooden, J.L. (2011). Thermometry of quartz mylonites: Importance of dynamic recrystallization on Ti-in-quartz reequilibration. Geochem., Geophy., Geosyst., v. 12(6).

Hanji, C.P., Sreenivasa, A. and Pujar, A.G. (2025). Quantitative Analysis of Finite Strain Accumulation and its Variation Across the Fold System in Southern Kaladgi Basin Around Bagalkot, India. Iranian Jour. Sci., v. 49(5), pp. 1267–1279.

Hentschel, F., Trepmann, C.A. and Janots, E. (2019). Deformation of feldspar at greenschist facies conditions – the record of mylonitic pegmatites from the Pfunderer Mountains, Eastern Alps. Solid Earth, v. 10(1), pp. 95–116.

Hirth, G. and Tullis, J. (1992). Dislocation creep regimes in quartz aggregates. Jour. Struct. Geol., v. 14(2), pp. 145–159.

Jayaprakash, A.V. (2007). Purana Basins of Karnataka– Geological Society of India. Geol. Surv. India, Kolkata, v. 129.

Jayaprakash, A.V., Sundaram, V., Hans, S.K. and Mishra, R.N. (1987). Geology of the Kaladgi–Badami Basin, Karnataka. *In*: Purana Basins of Peninsular India (Middle to Late Proterozoic), Radhakrishna, B.P. (*Ed.*), Geol. Soc. India, Bangalore, v. 6, pp. 201-226.

Jessell, M.W. (1987). Grain-boundary migration microstructures in a naturally deformed quartzite. Jour. Struct. Geol., v. 9(8), pp. 1007-1014.

Ji, S. (1998a). Deformation microstructure of natural plagioclase. *In*: Fault-Related Rocks, A Photographic Atlas, Snoke, A.W., Tullis, J.,Todd, V.R. (*Eds.*), Princeton University Press, New Jersey, pp. 276–277.

Ji, S. (1998b). Kink bands and recrystallization in plagioclase– In: Fault related rocks – a photographic atlas (Snoke, A., Tullis, J. and Todd, V.R., eds). Princeton University Press, New Jersey, pp. 278–279.

Kale, V.S. and Pillai, S. (2022). Sediments from Purana basins, India: Where were they derived from? Geosyst. Geoenviron., v. 1, pp. 69.

Kale, V., Nair, S. and Patil, S. (1998). Testimony of intraformational limestone breccias on Lokapur–Simikeri disconformity, Kaladgi Basin. Jour. Geol. Soc. India, v. 51(1), pp. 43-48.

Klepeis, K.A., Schwartz, J.J., Miranda, E., Lindquist, P., Jongens, R., Turnbull, R. and Stowell, H. (2022). The Initiation and Growth of Transpressional Shear Zones Through Continental Arc Lithosphere, Southwest New Zealand. Tectonics, v. 41(9).

Kruhl, J.H. (1996). Prism and basal plane parallel subgrain boundaries in quartz: a microstructural geothermobarometer. Jour. Meta. Geol., v. 14(5), pp. 581–589.

Lloyd, G.E. and Freeman, B. (1994). Dynamic recrystallization of quartz under greenschist conditions. Jour. Struct. Geol., v. 16(6), pp. 867–881.

Lychagin, D.V., Kungulova, E.N., Moskvichev, E.N., Tomilenko, A.A. and Tishin, P.A. (2020). Microstructure of Vein Quartz Aggregates as an Indicator of Their Deformation History: An Example of Vein Systems from Western Transbaikalia (Russia). Minerals, v. 10(10), pp.865. https://doi.org/10.3390/min10100865

Mainprice, D., Bouchez, J.L., Blumenfeld, P. and Tubià, J.M. (1986). Dominant c-slip in naturally deformed quartz: Implications for dramatic plastic softening at high temperature. Geologia, v. 14(10), pp. 819–822.

Mamtani, M.A. (2025). The Future of Structural Geology in the 21st Century – Moving from Mesoscale to Nanoscale Observations in Tectonically Deformed Rocks. Jour. Geol. Soc. India, v. 101(1), pp. 10–23.

Mukherjee, M.K., Das, S. and Modak, K. (2016). Basement–cover structural relationships in the Kaladgi Basin, southwestern India: indications towards a Mesoproterozoic gravity gliding of the cover along a detached unconformity. Precamb. Res., v. 281, pp. 495–520.

Mukherjee, M.K. and Modak, K. (2017). Structural Geometry and Deformation Patterns in Mesoproterozoic Cover Sediments of Kaladgi Basin: Implications for Exploration of Uranium and Hydrocarbons. Jour. Geosci. Res., v.1, pp. 217.

Mukherjee, M.K., Modak, K. and Ghosh, J. (2019). Illite crystallinity index from the Mesoproterozoic sedimentary cover of the Kaladgi basin, southwestern India: Implications on crustal depths of subsidence and deformation. Jour. Earth Syst. Sci., v. 128(4), pp. 101.

Nishikawa, O. and Takeshita, T. (1999). Dynamic analysis and two types of kink bands in quartz veins deformed under subgreenschist conditions. Tectonophysics, v. 301(1-2), pp. 21–34.

Papeschi, S. and Musumeci, G. (2019). Fluid□Assisted Strain Localization in Quartz at the Brittle/Ductile Transition. Geochem., Geophy., Geosyst., v. 20(6), pp. 3044–3064.

Passchier, C. (1982). Mylonitic deformation in the Saint-Barthélemy Massif, French Pyrenees, with emphasis on the genetic relationship between ultramylonite and pseudotachylyte. GUA Pap. Geol. Ser., v. 1(16), pp. 1-173.

Passchier, C.W. and Trouw, R.A.J. (2005). Microtectonics– Microtectonics. Springer-Verlag, Berlin/Heidelberg.

Petroccia, A., Giuntoli, F., Pilia, S., Viola, G., Sternai, P. and Callegari, I. (2025). Sustained strain localisation and coeval brittle-ductile deformation in an exhuming low-grade shear zone: Insights from the Saih Hatat Window (NE Oman). Jour. Struct. Geol., v. 191, pp. 105328.

Pillai, S. and Kale, V.S. (2019). Interplay Between Tectonics & Eustacy in a Proterozoic Epicratonic, Polyhistory Basin, North Dharwar Craton. *In*: Tectonics and Structural Geology: Indian Context, S. Mukherjee (*Ed.*), Springer, pp. 75–114.

Pillai, S. and Kale, V.S. (2021). Traverses Through the Bagalkot Group from North Karnataka State, India: Deformation in the Mesoproterozoic Supracrustal Kaladgi Basin. In: Geology, Mukherjee, S. (Ed.). Springer, Cham, v. 1, pp. 325–365.

Pryer, L.L. (1993). Microstructures in feldspars from a major crustal thrust zone: the Grenville Front, Ontario, Canada. Jour. Struct. Geol., v. 15(1), pp. 21–36.

Pujar, A., Puniya, M.K., Hiremath, M. and Anjanappa, S. (2021). Study of structural, deformation temperature, and strain analysis of the quartzarenites of south-central Kaladgi basin, exposed at and around Mullur ghat and Kallur village of Belgaum district, Karnataka, India. Arab. Jour. Geosci., v. 14(9), pp. 744.

Saintot, A., Stephenson, R., Brem, A., Stovba, S. and Privalov, V. (2003). Paleostress field reconstruction and revised tectonic history of the Donbas fold and thrust belt (Ukraine and Russia). Tectonics, v. 22(5).

Sigue, C., Suh, C.E. and Mbongue, J.L.N. (2023). Structural and microstructural evolution of Etam Shear Zone in the Central African Fold Belt, SW-Cameroon: implication of hydrothermal syn-tectonic quartz vein formation. Arab. Jour. Geosci., v. 16(5), pp. 341.

Simonetti, M., Carosi, R., Montomoli, C., Law, R.D. and Cottle, J.M. (2021). Unravelling the development of regional-scale shear zones by a multidisciplinary approach: The case study of the Ferriere-Mollières Shear Zone (Argentera Massif, Western Alps). Jour. Struct. Geol., v. 149, pp. 104399.

Stipp, M., Stünitz, H., Heilbronner, R. and Schmid, S.M. (2002). The eastern Tonale fault zone: a "natural laboratory" for crystal plastic deformation of quartz over a temperature range from 250 to 700 °C. Jour. Struct. Geol., v. 24(12), pp. 1861-1884.

Tullis, J. and Yund, A.R. (1987). Transition from cataclastic flow to dislocation creep of feldspar: mechanisms and microstructures. Geology, v. 15(7), pp. 606–609.

Urai, J.L., Means, W.D. and Lister, G.S. (1986). Dynamic recrystallization of minerals. *In*: Mineral and Rock Deformation: Laboratory Studies. Am. Geophy. Uni., v. 36, pp. 161–199.

Williams, M.L. and Burr, J.L. (1994). Preservation and evolution of quartz phenocrysts in deformed rhyolites from the proterozoic of south-western North America. Jour. Struct. Geol., v. 16(2), pp. 203–221.

Wu, S. and Groshong, R.H. (1991). Strain analysis using quartz deformation bands. Tectonophysics, v. 190(2-4), pp. 269–282.

Van Daalen, M., Heilbronner, R. and Kunze, K. (1999). Orientation analysis of localized shear deformation in quartz fibres at the brittle-ductile transition. Tectonophysics, v. 303(1-4), pp. 83-107.